

## Predicting the rate of microbial respiration in geochemical environments

QUSHENG JIN and CRAIG M. BETHKE\*

Department of Geology, 1301 W Green Street, 245 Natural History Building, University of Illinois, Urbana, IL 61801-2919, USA

(Received August 11, 2003; accepted in revised form August 12, 2004)

**Abstract**—A new rate law of general form can be applied to predict rates of microbial respiration in various geochemical environments. Because it accounts for the energy available to a microbe, the rate law can be applied in over a spectrum of conditions, ranging from environments rich in chemical energy to those fully oligotrophic. Two sets of parameters, one related to thermodynamic constraints and the other set appearing in kinetic terms, need be determined to apply the new law. We show that the thermodynamic parameters can be estimated from knowledge of the details of a microbe's respiratory chain. The kinetic parameters are best determined by fitting the rate law to experimental observations. We find that for respiration characterized by a strong thermodynamic driving force, such as many types of aerobic respiration and denitrification, the kinetic controls on respiration rate almost invariably dominate. In such cases, the thermodynamic control can safely be ignored. For respiration utilizing less powerful thermodynamic driving forces, such as sulfate reduction and reductive methanogenesis, the thermodynamic control on respiration rate can be dominant. It is of critical importance in these cases to account for thermodynamic as well as kinetic controls when calculating respiration rates. Taking as examples methanogenesis and sulfate reduction in hydrothermal fluids, we show how the new rate law can be applied over a spectrum of conditions and energy availability. *Copyright* © 2005 Elsevier Ltd

### 1. INTRODUCTION

Respiring microorganisms inhabit much of the Earth's hydrosphere and lithosphere, thriving in environments ranging from surface water to submarine hot springs to groundwater several kilometers below the surface (Jones et al., 1983; Jannasch and Mottl, 1985; Stevens and Mckinley, 1995). Such microbes derive the energy they need to live, grow, and reproduce from their chemical environments, by transferring electrons from reduced to oxidized chemical species. The chemical environment, therefore, affects a microbe's respiration, and respiration alters the chemical environment.

The single most significant issue arising in quantifying the relationship between a respiring microbe and its environment is predicting the microbe's respiration rate, i.e., the rate at which it consumes its substrate as it transfers electrons through its electron transport chain. Each of the rate equations in common use in microbial kinetics today—the Monod and dual Monod equations, for example—treats microbial respiration as a unidirectional, autocatalytic reaction. In other words, the microbe conserves energy liberated by catalyzing the forward progress of respiration. It uses the conserved energy to grow and reproduce, increasing the amount of biomass available for further catalysis.

The rate equations in common use are limited in several ways. They are not general, in the sense that they do not consider all of the chemical species consumed and liberated by the electron donating and accepting half-reactions. They account for only forward progress of respiration, although any enzyme catalyzes a reaction in both the forward and reverse directions simultaneously, albeit not necessarily at equal rates. Finally, the equations do not account for the thermodynamic

requirement that a microbe conserve energy from its environment.

In recent papers (Jin and Bethke, 2002, 2003), we developed a general rate law predicting the rate of electron flow through the transport chain of respiring organisms. The rate law was derived on the basis of irreversible thermodynamics and the chemiosmotic model, which holds that a cell (or a mitochondrion in an eukaryotic cell) conserves some of the energy released as electrons pass through its respiratory chain, from an electron donating to an electron accepting half-reaction. The new law predicts that the rate of microbial respiration varies with the product of three terms: a kinetic factor describing the effect of the electron donating half-reaction, a similar factor for the electron accepting half-reaction, and a thermodynamic potential factor. The latter term accounts for the availability of energy in the geochemical environment.

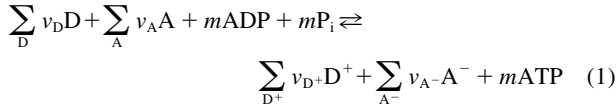
The new rate law differs from the rate laws in common use today in its generality. Kinetic factors in the new rate law account for the concentration of each chemical species involved in microbial respiration, and the thermodynamic potential factor allows the rate law to be applied across a spectrum of energy availability. As we discuss in this paper, these generalities are critical for predicting the rate of microbial respiration in geochemical environments, such as degradation of organic compounds using various terminal electron accepting processes in soils, sediments, and water bodies.

In this paper, we discuss how to account for thermodynamic control in predicting rates of microbial respiration in geochemical environments, paying special attention to the question of determining the parameters needed to evaluate the rate law. Using hydrothermal systems as an example, we show how rate expressions can be developed from a general rate law and how various factors control the rates of hydrogenotrophic methanogenesis and acetotrophic sulfate reduction.

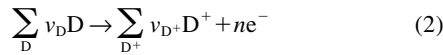
\* Author to whom correspondence should be addressed (bethke@uiuc.edu).

## 2. RATE LAW FOR MICROBIAL RESPIRATION

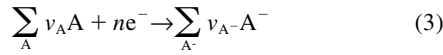
Respiring microorganisms derive energy for growth from their chemical environments. In our previous work (Jin and Bethke, 2002, 2003), we represented microbial respiration as a coupled process between redox reaction and ATP synthesis,



where  $\nu_{\text{D}}$ , etc., are reaction coefficients,  $m$  is the number of ATPs synthesized,  $\text{P}_i$  is the phosphate ion,  $\text{D}^+$  and  $\text{D}$  are chemical species on the oxidized and reduced sides of the donating half-reaction,



$\text{A}$  and  $\text{A}^-$  are chemical species on the oxidized and reduced sides of the accepting-half reaction,



Here coefficient  $n$  is the number of electrons transferred per turnover of the reaction. Electron transfer between the donating and accepting half-reaction releases Gibbs free energy  $\Delta G_{\text{redox}}$

$$\Delta G_{\text{redox}} = \Delta G_{\text{redox}}^{\circ} + RT \ln \frac{\prod_{\text{D}^+} a_{\text{D}^+}^{\nu_{\text{D}^+}} \prod_{\text{A}^-} a_{\text{A}^-}^{\nu_{\text{A}^-}}}{\prod_{\text{D}} a_{\text{D}}^{\nu_{\text{D}}} \prod_{\text{A}} a_{\text{A}}^{\nu_{\text{A}}}} \quad (4)$$

where  $\Delta G_{\text{redox}}^{\circ}$  is the standard Gibbs free energy change of reaction,  $a_{\text{D}}$ , etc., are species activities,  $R$  is the gas constant, and  $T$  is the absolute temperature. In evaluating Eqn. 4, it is a common practice in microbiology to use concentration ( $[\text{D}]$ , etc.) and partial pressure instead of activity ( $a_{\text{D}}$ , etc.) and fugacity.

Microorganisms can conserve part of the energy available ( $-\Delta G_{\text{redox}}$ ) by synthesizing ATP (reaction 1). The free energy change in synthesizing ATP from ADP and  $\text{P}_i$ , the phosphorylation potential  $\Delta G_{\text{p}}$ , is  $\sim 50$  kJ per mol ATP under typical cellular conditions (White, 1995). Since  $m$  ATPs are synthesized, the total energy saved is  $m \Delta G_{\text{p}}$ . The sum  $\Delta G_{\text{redox}} + m \Delta G_{\text{p}}$ , therefore, is the free energy change of microbial respiration (reaction 1) and its negative value is the thermodynamic driving force.

The net respiration rate  $r$  ( $\text{M s}^{-1}$ ) is

$$r = -\frac{1}{\nu_{\text{D}}} \frac{d[\text{D}]}{dt} = -\frac{1}{\nu_{\text{A}}} \frac{d[\text{A}]}{dt} = \frac{1}{\nu_{\text{D}^+}} \frac{d[\text{D}^+]}{dt} = \frac{1}{\nu_{\text{A}^-}} \frac{d[\text{A}^-]}{dt} \quad (5)$$

which is described by the rate law

$$r = k[\text{X}] F_{\text{D}} F_{\text{A}} F_{\text{T}} \quad (6)$$

where  $k$  is a rate constant,  $[\text{X}]$  is biomass concentration,  $F_{\text{D}}$  and  $F_{\text{A}}$  are kinetic factors accounting for concentrations of chemical species involved in the donating and accepting half-reactions, and  $F_{\text{T}}$  is the thermodynamic potential factor accounting for the effect of the thermodynamic driving force. The kinetic factors are expressed

$$F_{\text{D}} = \frac{\prod_{\text{D}} [\text{D}]^{\beta_{\text{D}}}}{\prod_{\text{D}} [\text{D}]^{\beta_{\text{D}}} + K_{\text{D}} \prod_{\text{D}^+} [\text{D}^+]^{\beta_{\text{D}^+}}} \quad (7)$$

and

$$F_{\text{A}} = \frac{\prod_{\text{A}} [\text{A}]^{\beta_{\text{A}}}}{\prod_{\text{A}} [\text{A}]^{\beta_{\text{A}}} + K_{\text{A}} \prod_{\text{A}^-} [\text{A}^-]^{\beta_{\text{A}^-}}} \quad (8)$$

Here,  $\beta_{\text{D}}$ , etc., are exponents applied to concentration values, and  $K_{\text{D}}$  and  $K_{\text{A}}$  are constants, the values of which depend on details of the electron transport chain. The thermodynamic potential factor  $F_{\text{T}}$  is given as a function of the driving force as

$$F_{\text{T}} = 1 - \exp\left(\frac{\Delta G_{\text{redox}} + m \Delta G_{\text{p}}}{\chi RT}\right) \quad (9)$$

where  $\chi$  is the average stoichiometric number for the overall reaction (reaction 1).

## 3. PARAMETER DETERMINATION

The new rate law (Eqns. 6, 7, 8, and 9), because of its generality, contains more parameters than are needed to evaluate any of the simple rate laws in common use today. This requirement is not a limitation of the new law; instead, it allows a rate theory valid over specific conditions to be derived from the general case, and for a general expression to be developed, where sufficient data are available. In this section, we discuss how the various parameters in the new rate law can be determined.

To apply the new rate law in its most general form, we need to determine values for (1) the parameters  $k$ ,  $K_{\text{D}}$ ,  $K_{\text{A}}$ , the exponents  $\beta_{\text{D}}$ ,  $\beta_{\text{A}}$ , and so on, which appear in the kinetic factors, and (2) the number  $m$  of ATPs synthesized and the average stoichiometric number  $\chi$ , which arise in the expression for the thermodynamic potential factor  $F_{\text{T}}$ . We refer to these groups as the kinetic parameters and thermodynamic parameters, respectively.

### 3.1. Kinetic Parameters

The kinetic parameters cannot be determined for real problems from first principles, but must be estimated by fitting the rate expression to experimental observations. Most microbial respiration experiments are run in a batch reactor, and the results recorded as variation in the concentrations of chemical species and biomass with time (e.g., Simkins and Alexander, 1984). In fitting the data, the rate constant  $k$  determines how rapidly the concentrations of chemical species change, per unit biomass concentration, and the values of  $K_{\text{D}}$  and  $K_{\text{A}}$  affect the shape of these curves. Specifically, increasing  $K_{\text{D}}$  and  $K_{\text{A}}$  works to decrease the convexity of the curves.

It is worth noting that the kinetic terms

$$K_{\text{D}} \prod_{\text{D}^+} [\text{D}^+]^{\beta_{\text{D}^+}}$$

and

$$K_{\text{A}} \prod_{\text{A}^-} [\text{A}^-]^{\beta_{\text{A}^-}}$$

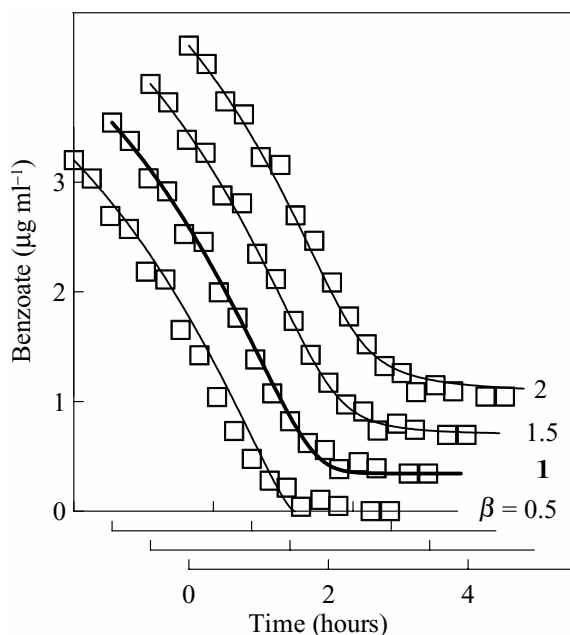


Fig. 1. Fitting of a kinetic rate law (Eqn. 10) to the observed evolution of benzoate concentration in a laboratory experiment reported by Simkins and Alexander (1984). Taking the exponent  $\beta$  to be 0.5, 1, 1.5, and 2 shows that such data fitting can be largely insensitive to the value chosen for this parameter. In evaluating the rate law, we assume values of  $2.0 \times 10^{-6} \text{ mol g}^{-1} \text{ s}^{-1}$  and  $3.14 \times 10^{-6} \text{ M}$  for  $k$  and  $K_D$ , respectively. To account for biomass growth, we assume a decay constant of zero and calculate rates of biosynthesis as a product of growth yield  $Y$  and respiration rate  $r$ . We take the initial biomass as  $0.92 \text{ mg L}^{-1}$  and a growth yield of 60 g biomass per mol benzoate (Jin and Bethke, 2003).

which occupy the position of the half-saturation constants in the Monod and dual-Monod equations, may differ in value from those constants. In fitting the new law to experimental data, we account for both kinetic and thermodynamic factors, whereas the Monod equations carry only kinetic terms. The kinetic terms, therefore, can be expected to be equivalent to the half-saturation constants only where the thermodynamic potential factor remains close to unity.

There is little theoretical guidance for choosing values for the exponents  $\beta_D$ ,  $\beta_A$ , and so on. Like  $K_D$  and  $K_A$ , it is best to derive these values through the analysis of experimental results, although this process is not always straightforward. As pointed out by Masel (2001), variation in a batch reactor of species concentration with time is not always sensitive to the value chosen for the exponents. To show this point, we take as example the results of a study of benzoate degradation reported by Simkins and Alexander (1984) and fit by visual inspection the simple rate expression.

$$r = k[X] \frac{[D]^\beta}{[D]^\beta + K_D} \quad (10)$$

to the reported variation with time in benzoate concentration. As shown in Figure 1, curves for  $\beta$  values of 0.5, 1, 1.5, and 2 fit the data almost equally well.

In our experience, it is in many cases acceptable to assign values of unity to the exponents, as we will assume hereafter in

this paper. The parameter may in fact be equal to one, which is certainly not uncommon in chemical kinetics. However, the reader should keep in mind that this assumption is not necessarily true, and that it may be necessary to consider nonlinear exponents in applying rate laws over the broad range of chemical conditions encountered in nature.

### 3.2. Thermodynamic Parameters

The average stoichiometric number  $\chi$  and the number  $m$  of ATPs synthesized per reaction turnover can be estimated from knowledge of the functioning of the respiratory chain. The value of  $\chi$  can be taken as the number of times the rate determining step occurs in the overall reaction (reaction 1). The rate determining step is typically a step associated with energy conservation, generally proton translocation across the cell membrane (Mitchell, 1961). In the examples below, we show how the values of  $\chi$  and  $m$  can be estimated for dihydrogen-respiring microbes using various electron acceptors (Table 1).

The values of  $\chi$  and  $m$  are in general proportional to the number  $n$  of electrons transferred in the overall reaction. In other words, they depend on how we choose to write the reaction. For consistency, we will express  $\chi$  and  $m$  per  $\text{H}_2$  oxidized, which is per pair of electrons transferred ( $n = 2$ ). We will also assume that passage of three protons through the ATP synthase enzyme, from outside to inside the cell membrane, is required to produce each ATP.

For the case of dioxygen serving as the electron acceptor,  $\sim 3$  protons are translocated per electron transferred through the respiratory chain (van Verseveld and Bosma, 1987; Stouthamer, 1991), two of which are translocated at the rate limiting step (Erecinska and Wilson, 1982). The value of  $m$ , then, is two, since making each ATP requires three protons, and we have written the reaction for the transfer of two electrons. The value of  $\chi$  is 4, because the rate limiting step occurs twice for each of the two electrons transferred.

In denitrification, nitrate is first reduced to nitrite, then to nitric oxide, nitrous oxide, and finally to dinitrogen. Two protons are translocated in each instance of the quinone cycle in the respiratory chain (Trumpower, 1990), with each instance consuming one  $\text{H}_2$ . The quinone cycle occurs once when nitrate is reduced to nitrite, and again during each of the three subsequent reductions (Stouthamer, 1991). The value of  $m$  for denitrification, then, is  $2/3$ , i.e., two protons are translocated per pair of electrons transferred, and three are required to make one ATP.

In sulfate reduction, experimental observation (Nethen-Jaenchen and Thauer, 1984) has shown the value of  $m$  to be  $1/3$ . In hydrogenotrophic methanogenesis,  $\text{CO}_2$  and  $\text{H}_2$  react to form  $\text{CH}_4$  via the  $\text{CO}_2$  reduction pathway. It is difficult to figure an appropriate value of  $m$  for this respiration directly, because details of the respiratory chain are poorly known. We have obtained good results by assuming that  $1/3$  of a proton is translocated per electron transferred, which leads to a value of  $2/9$  for  $m$ . This value is close to that observed for sulfate reduction, consistent with the fact that for the two types of respiration the energies  $\Delta G_{\text{redox}}$  are similar.

In anaerobic respiration, energy is conserved by the quinone cycle. Two protons are translocated in each instance of the quinone cycle in the respiratory chain (Trumpower, 1990), with

Table 1. Thermodynamic parameters for dihydrogenotrophy using various terminal electron accepting processes common in the geochemical environment.

	$\Delta E^{\circ'}$ (V) <sup>a</sup>	$\chi$ <sup>b</sup>	$m$ <sup>b</sup>
Oxygen respiration ( <i>Paracoccus denitrificans</i> <sup>c</sup> ) $\text{H}_2 + \frac{1}{2} \text{O}_2 \rightleftharpoons \text{H}_2\text{O}$	1.23	4	2
Denitrification ( <i>Paracoccus denitrificans</i> ) $\text{H}_2 + \frac{2}{5} \text{NO}_3 + \frac{2}{5} \text{H}^+ \rightleftharpoons \frac{1}{5} \text{N}_2 + \frac{6}{5} \text{H}_2\text{O}$	1.2	2	2/3
Sulfate reduction ( <i>Desulfovibrio vulgaris</i> ) $\text{H}_2 + \frac{1}{4} \text{H}^+ + \frac{1}{4} \text{SO}_4^{2-} \rightleftharpoons \frac{1}{4} \text{HS}^- + \text{H}_2\text{O}$	0.193	2	1/3
Methanogenesis $\text{H}_2 + \frac{1}{4} \text{H}^+ + \frac{1}{4} \text{HCO}_3^- \rightleftharpoons \frac{1}{4} \text{CH}_4 + \frac{3}{4} \text{H}_2\text{O}$	0.17	2	2/9

<sup>a</sup> Data from Thauer et al. (1977);  $\Delta E^{\circ'}$  represents the redox potential difference at the biological standard state: 25°C, pH 7, and chemical species concentration of 1 M.

<sup>b</sup> Values of  $\chi$  and  $m$  depend on the number of electrons transferred; here reactions are written so that  $n$  is 2.

<sup>c</sup> Microbial species in parentheses are examples of organisms whose respiration is consistent with the values shown for  $\chi$  and  $m$ .

each instance consuming one  $\text{H}_2$ . Making the logical assumption that the quinone cycle is the rate determining step, the value of  $\chi$  per  $\text{H}_2$  oxidized for anaerobic respiration is 2. In other words, proton translocation during the quinone cycle occurs twice per pair of electrons transferred.

#### 4. THERMODYNAMIC POTENTIAL FACTOR

The rate law described in this paper is unique in that it incorporates a thermodynamic potential factor  $F_T$ . This factor describes how respiration rate varies with the energy available ( $-\Delta G_{\text{redox}}$ ) in a microbe's environment, accounting for the energy the cell conserves as ATP. It is a nonlinear function of the thermodynamic driving force, the difference between the energy liberated by electron transfer (the energy available) and that conserved ( $m \times \Delta G_p$ ) by the microbe (Fig. 2). Where the energy available is large relative to the amount conserved, the thermodynamic driving force is large and the value of  $F_T$  approaches one. In this case, the thermodynamic potential factor need not be carried in the rate calculation. Where the energy available falls close to the energy conserved, the thermodynamic driving force is smaller and  $F_T$  assumes a value less than one.

The thermodynamic factor, in this case, can exert a significant control on the respiration rate and needs to be considered in predicting the rate. Where the energy available balances the energy conserved, microbial respiration (reaction 1) reaches a state of thermodynamic equilibrium, and the driving force and  $F_T$  are zero. The respiration rate then takes a value of zero (Eqn. 6), reflecting a cessation of respiration. Where the energy available is less than the energy required to synthesize ATP, the driving force as well as  $F_T$  become negative, implying that respiration will proceed backwards. In reality, to prevent unnecessary dissipation of ATP, the cell may regulate its respiratory chain to prevent such reverse electron transfer.

Because the new rate law incorporates this factor, it can be applied across a spectrum of thermodynamic conditions. This

capacity is significant in light of the broad range of energy availability in natural environments. The energy available ( $-\Delta G_{\text{redox}}$ ) to a microbe in the natural environment depends in large part on the terminal electron accepting process the microbe uses. Taking as examples various terminal electron accepting processes using dihydrogen, i.e.,  $\text{H}_2(\text{aq})$ , as electron donor (Table 1), Figure 3 shows how the energy available and the corresponding thermodynamic potential factor varies with dihydrogen concentration in a typical geochemical environment.

From this plot, it is clear that large amounts of energy per mole of dihydrogen consumed are available for the processes of aerobic respiration and denitrification. The aerobic respiration of dihydrogen proceeds according to

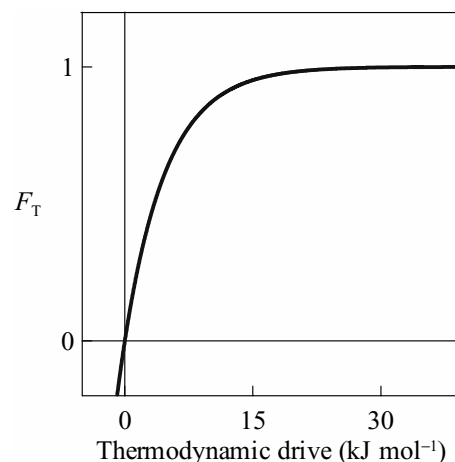


Fig. 2. Variation with thermodynamic driving force of the thermodynamic potential factor  $F_T$  for anaerobic respiration. The line was calculated using Eqn. 9, taking a value for  $\chi$  of 2, which typical for an anaerobic respiration reaction written in terms of the transfer of two electrons ( $n = 2$ ).

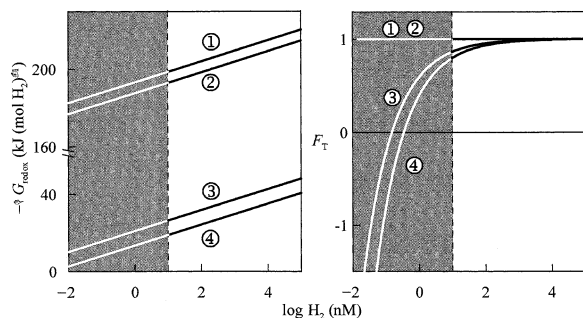
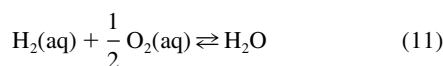


Fig. 3. Dependence on dihydrogen concentration of the energy available ( $-\Delta G_{\text{redox}}$ ; on left) and thermodynamic potential factor  $F_T$  (right) for aerobic respiration (line 1), denitrification (line 2), sulfate reduction (line 3) and methanogenesis (line 4) in a typical geochemical environment. We assume a temperature of 10°C, pH of 7,  $[\text{O}_2]$  of 10 nM,  $\text{N}_2$  partial pressure of 0.7 atm,  $[\text{NO}_3^-]$  of 1 mM,  $[\text{SO}_4^{2-}]$  of 5 mM,  $[\text{HS}^-]$  of 1  $\mu\text{M}$ ,  $[\text{HCO}_3^-]$  of 30 mM, and  $[\text{CH}_4]$  of 10  $\mu\text{M}$ . The shaded area indicates the approximate range of  $[\text{H}_2]$  commonly observed in near-surface natural environments.



in which two electrons ( $n = 2$ ) are transferred. As we discussed previously, the values of  $\chi$  and  $m$  for aerobic respiration are 4 and 2, respectively. Substituting into Eqn. 9, we can write the thermodynamic potential factor as

$$F_T = 1 - \exp\left(\frac{\Delta G_{\text{redox}} + 2\Delta G_p}{4RT}\right) \quad (12)$$

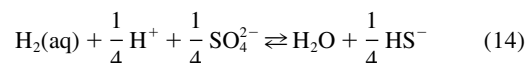
The energy available  $-\Delta G_{\text{redox}}$  can be calculated according to

$$\Delta G_{\text{redox}} = \Delta G_{\text{redox}}^{\circ} + RT \ln[\text{H}_2]^{-1}[\text{O}_2]^{-1/2} \quad (13)$$

Taking  $\Delta G_p$  as 50 kJ (mol ATP) $^{-1}$ , the amount of energy conserved ( $2 \Delta G_p$ ) then is 100 kJ (mol  $\text{H}_2$ ) $^{-1}$ . Under the conditions considered, the value of  $-\Delta G_{\text{redox}}^{\circ}$  equals 263.9 kJ (mol  $\text{H}_2$ ) $^{-1}$ , which is considerably larger than the energy conserved, 100 kJ mol $^{-1}$ . As such, the thermodynamic driving force is large and the thermodynamic potential factor takes on a value of one.

The thermodynamic drive depends on the abundance of  $\text{H}_2$  and  $\text{O}_2$  (Eqn. 13), but for a broad range of the concentrations of these species the energy  $-\Delta G_{\text{redox}}$  available greatly exceeds that conserved. Taking a small dioxygen concentration of 10  $\mu\text{M}$ , for example, the energy available ranges from 180 to 210 kJ mol $^{-1}$  where dihydrogen concentration ranges from 0.01 nM to 1 mM. As a result, the driving force for reaction 11 is almost invariably large and the value of the thermodynamic potential factor remains near unity (Fig. 3). The thermodynamic control, therefore, can almost always be neglected in predicting the rate of the aerobic respiration of dihydrogen. A parallel analysis of microbial denitrification (Table 1) similarly shows that the value of  $F_T$  approaches one under most geochemical conditions, so that the thermodynamic control can commonly be neglected.

In the case of sulfate reduction using dihydrogen as electron donor,



we can write the thermodynamic potential factor as

$$F_T = \left[ 1 - \exp\left(\frac{\Delta G_{\text{redox}} + \frac{1}{3} \Delta G_p}{2RT}\right) \right] \quad (15)$$

since, as already discussed, appropriate values for  $\chi$  and  $m$  for reaction 14 are 2 and 1/3, respectively. Taking the phosphorylation potential  $\Delta G_p$  as 50 kJ (mol ATP) $^{-1}$ , the energy conserved ( $m\Delta G_p$ ) is  $\sim 17$  kJ (mol  $\text{H}_2$ ) $^{-1}$ . From Eqn. 15, the value of  $F_T$  approaches unity where the thermodynamic driving force is larger than  $\sim 15$  kJ mol $^{-1}$  (Fig. 2). In other words, where the energy available from reaction 14 is greater than  $\sim 32$  kJ mol $^{-1}$ ,  $F_T$  approaches unity and the thermodynamic control can be neglected when predicting the rate of sulfate reduction.

We can calculate the energy available  $-\Delta G_{\text{redox}}$  from the relation

$$\Delta G_{\text{redox}} = \Delta G_{\text{redox}}^{\circ} + RT \ln \frac{[\text{HS}^-]^{1/4}}{[\text{H}_2][\text{H}^+]^{1/4}[\text{SO}_4^{2-}]^{1/4}} \quad (16)$$

where the standard Gibbs free energy change  $\Delta G_{\text{redox}}^{\circ}$  is  $-65.46$  kJ (mol  $\text{H}_2$ ) $^{-1}$  at 10°C. Since this value is small, the energy available  $-\Delta G_{\text{redox}}$  depends significantly on the abundance of reactant species  $\text{H}_2$  and  $\text{SO}_4^{2-}$ , and the extent to which the product species  $\text{HS}^-$  has accumulated. In natural environments, commonly observed dihydrogen concentrations range from less than 1 nM to  $\sim 10$  nM (Lovley and Goodwin, 1988). Assuming a typical value for  $[\text{SO}_4^{2-}]$  of 5 mM,  $[\text{HS}^-]$  of 1  $\mu\text{M}$ , and a pH of 7, the energy available ( $-\Delta G_{\text{redox}}$ ) is less than 26 kJ mol $^{-1}$ . Under such conditions, the value of  $F_T$  is less than one and thermodynamics, therefore, exerts an important control on the rate of sulfate reduction. The thermodynamic drive for reductive methanogenesis, by similar analysis, is commonly small enough that the thermodynamic potential factor  $F_T$  can vary sharply below one, and hence must be considered to predict the rate of methanogenesis.

## 5. APPLICATION

The new rate law offers the potential of working over a spectrum of available energy, from fully oligotrophic environments to those rich in chemical energy. In this section, we consider how the new rate law can be applied to predict rates of methanogenesis and sulfate reduction at seafloor hydrothermal vents, where hot hydrothermal fluid mixes with cold seawater. A number of previous studies of the geomicrobiology of these hydrothermal ecosystems have focused on calculating the Gibbs free energy for various metabolisms (McCollom and Shock, 1997), culturing organisms sampled there (Kashefi et al., 2003), and the molecular biology of the sites (Reysenbach et al., 2000). Here, we extend those studies to show how microbial respiration rates might vary there during the mixing process, according to our rate law.

A typical seafloor hydrothermal fluid is acidic and rich in dissolved sulfide and dihydrogen. Seawater is slightly alkaline and almost devoid of sulfide and dihydrogen (Table 2). Where

Table 2. Properties and concentrations of various species in a mid-ocean ridge hydrothermal fluid, East Pacific Rise near 21°N, and in seawater.<sup>a</sup>

Species	Hydrothermal fluid	Seawater
O <sub>2</sub>	0	0.123 mM
SO <sub>4</sub> <sup>2-</sup>	0	29.5 mM
HCO <sub>3</sub> <sup>-</sup>	2 mM	2.4 mM
HS <sup>-</sup>	6.81 mM	0
H <sub>2</sub> (aq)	1.7 mM	0
Acetate	0.02 mM	0
CH <sub>4</sub>	0.07 mM	0
T (°C)	273	4
pH	4.2	8.1

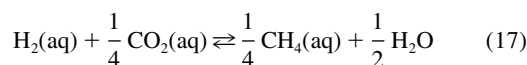
<sup>a</sup> Acetate concentration is assumed based on experiment results under hydrothermal conditions (Huber and Wächtershäuser, 1997); for other concentrations assumed in the calculations, refer to Bethke (1996, table 16.3).

hot hydrothermal fluid mixes with cold seawater, the combination of reduced and oxidizing species creates rich sources of energy for chemolithotrophic microorganisms. To understand how methanogens and sulfate reducing bacteria exploit this chemical energy, we model the mixing of hydrothermal fluid at East Pacific Rise near 21°N with seawater using program React from the Geochemist's Workbench software package (Bethke, 2002); the input file is available in the electronic annex.

Our modeling approach is similar to that described in Bethke (1996, chap. 16.2) except that we hold methane in redox disequilibrium with carbonate, sulfide in disequilibrium with sulfate, acetate in disequilibrium with bicarbonate, and dihydrogen in disequilibrium with hydrogen ions. We assume that microbial respiration is sufficiently slow as not to significantly affect species concentrations in the rapidly mixing fluid. Figure 4 shows how temperature, and the concentrations of key chemical species change as seawater mixes into the hydrothermal fluid. Over the course of the mixing reaction, temperature, pH, and the concentrations of dihydrogen, acetate, methane, and sulfide decrease, whereas the sulfate concentration and pH increase.

### 5.1. Methanogenesis

Where seawater reacts with hydrothermal fluids, hydrogenotrophic methanogens can conserve energy by producing CH<sub>4</sub> from CO<sub>2</sub> and dihydrogen, using the CO<sub>2</sub>-reduction pathway (Deppenmeier et al., 1996)



The free energy  $\Delta G_{\text{redox}}$  released by this reaction depends on its standard Gibbs free energy change  $\Delta G_{\text{redox}}^\circ$ , temperature, and the concentrations of dihydrogen, carbon dioxide, and methane, according to

$$\Delta G_{\text{redox}} = \Delta G_{\text{redox}}^\circ + RT \ln \frac{[\text{CH}_4]^{1/4}}{[\text{H}_2][\text{CO}_2]^{1/4}} \quad (18)$$

As shown in Figure 5, the value of  $\Delta G_{\text{redox}}^\circ$  varies with temperature, increasing (becoming less negative) with increasing temperature.

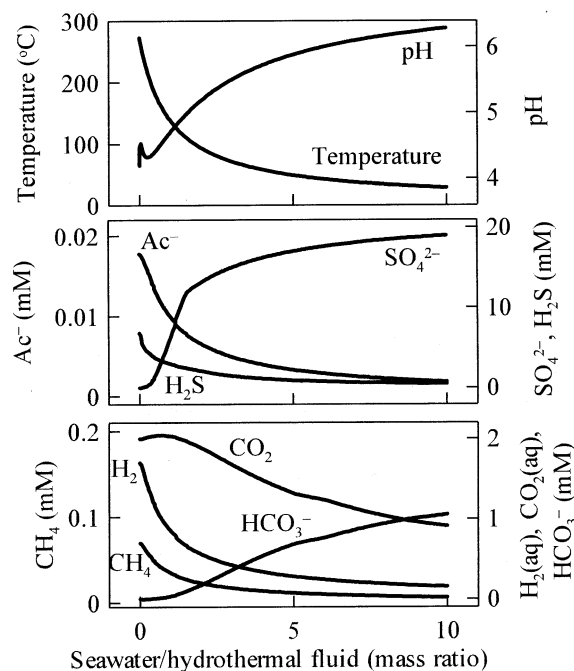


Fig. 4. Variation in temperature, pH, and the concentrations of various species as seawater mixes into and reacts with fluid from a seafloor hydrothermal vent, as calculated by a reaction model. Initial concentrations of chemical species in the two fluids are listed in Table 2.

From Eqn. 18, we see that several factors affect the energy available for methanogenesis during mixing. As cold seawater mixes into the hydrothermal fluid, the decreasing temperature drives an increase in the value of  $-\Delta G_{\text{redox}}^\circ$  (i.e.,  $\Delta G_{\text{redox}}^\circ$  becomes more negative), which in turn increases the energy available  $-\Delta G_{\text{redox}}$ . Variation in the concentrations of the dissolved gases, which may serve to increase or decrease the energy available, has an effect secondary to that of temperature.

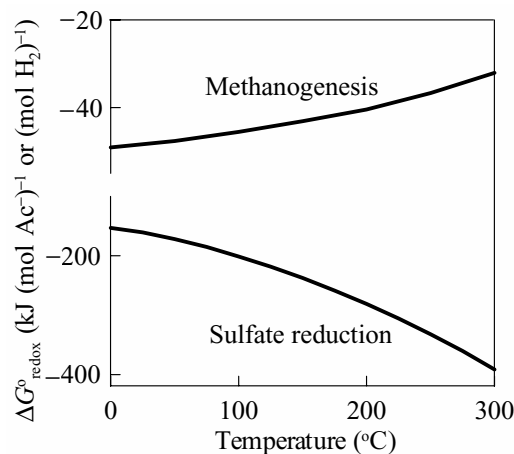


Fig. 5. Variation with temperature of the standard Gibbs free energy change ( $\Delta G_{\text{redox}}^\circ$ ) of hydrogenotrophic methanogenesis (reaction 17) and acetotrophic sulfate reduction (reaction 27). Values of  $\Delta G_{\text{redox}}^\circ$  were calculated vs. temperature using the Geochemist's Workbench (Bethke, 1996).

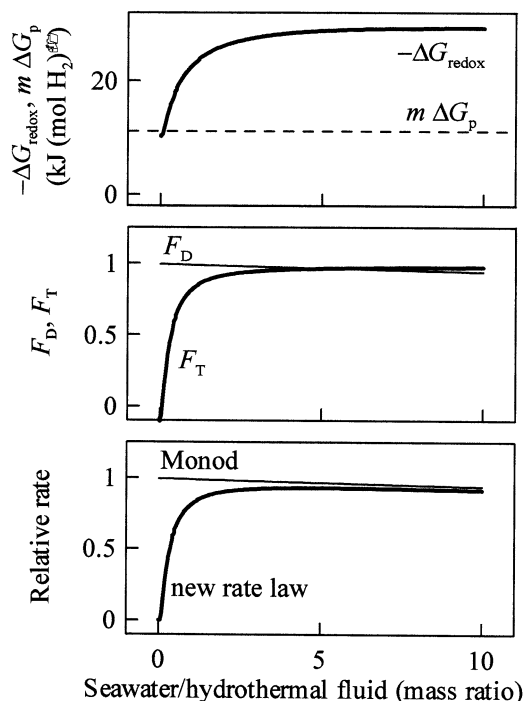


Fig. 6. Variation in the energy available  $-\Delta G_{\text{redox}}$ , thermodynamic potential factor  $F_T$ , kinetic factor  $F_D$ , and relative respiration rate of hydrogentrophic methanogenesis during mixing of seawater with a seafloor hydrothermal fluid. The dashed line indicates the energy conserved ( $m\Delta G_p$ ). The value of  $F_T$  is evaluated using Eqn. 19, and  $F_D$  using Eqn. 25. Respiration rates are predicted using the Monod equation (Eqn. 25) and the new rate law (Eqn. 26), respectively. In evaluating Eqns. 25 and 26, we neglect the effect of  $[\text{H}^+]$ ,  $[\text{CO}_2]$ , and  $[\text{CH}_4]$ , and take the value of  $K'_D$  as  $5.0 \times 10^{-3}$  mM. Relative respiration rate, which is unitless, is the actual rate  $r$  divided by  $k[\text{X}]$ .

As a result, the energy available increases as the fluid cools during mixing (Fig. 6).

As discussed previously, the values of  $\chi$  and  $m$  for reaction 17 are 2 and 2/9, respectively. Substituting into Eqn. 9 gives the thermodynamic potential factor

$$F_T = 1 - \exp\left(\frac{\Delta G_{\text{redox}} + \frac{2}{9}\Delta G_p}{2RT}\right) \quad (19)$$

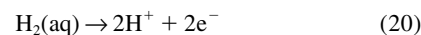
McKay et al. (1982) noted that at hydrothermal temperatures the value of phosphorylation potential  $\Delta G_p$  remains near 50 kJ (mol ATP) $^{-1}$ . Assuming that under hydrothermal conditions methanogens use the same type of respiratory chain as at room temperature (i.e.,  $m$  is same), the amount of energy conserved,  $m\Delta G_p$ , then, is  $\sim 11$  kJ (mol  $\text{H}_2$ ) $^{-1}$ . The value of  $F_T$  approaches unity where the thermodynamic driving force ( $-\Delta G_{\text{redox}} - m\Delta G_p$ ) is larger than  $\sim 15$  kJ mol $^{-1}$  (Fig. 2). With this in mind, we see the value of  $F_T$  approaches unity where the energy available  $-\Delta G_{\text{redox}}$  from reaction 17 is greater than  $\sim 26$  kJ (mol  $\text{H}_2$ ) $^{-1}$ ; only under these conditions can the term be ignored safely in evaluating the rate expression.

During the mixing process, the calculated energy available increases from a value of 10 kJ (mol  $\text{H}_2$ ) $^{-1}$  in the fluid before mixing to over 26 kJ (mol  $\text{H}_2$ ) $^{-1}$  at a mixing ratio of about two

parts seawater to one part hydrothermal fluid (Fig. 6). The value of  $F_T$  is almost zero in the unmixed hydrothermal fluids. As the fluids mix, the value of  $F_T$  increases and approaches unity, reflecting the increasing energy available.

## 5.2. Rate of Methanogenesis

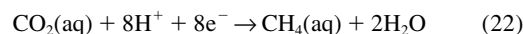
To predict the rate of methanogenesis using the new rate law, we can write kinetic factor  $F_D$  for the electron donating half-reaction,



according to Eqn. 7, which gives

$$F_D = \frac{[\text{H}_2]}{[\text{H}_2] + K_D[\text{H}^+]} \quad (21)$$

Similarly, from the accepting half-reaction



and the form of Eqn. 8,  $F_A$  can be written

$$F_A = \frac{[\text{CO}_2][\text{H}^+]}{[\text{CO}_2][\text{H}^+] + K_A[\text{CH}_4]} \quad (23)$$

The complete rate expression for hydrogentrophic methanogenesis, then, is given as

$$r = k[\text{X}] \frac{[\text{H}_2]}{[\text{H}_2] + K_D[\text{H}^+]} \frac{[\text{CO}_2][\text{H}^+]}{[\text{CO}_2][\text{H}^+] + K_A[\text{CH}_4]} F_T \quad (24)$$

by substituting Eqns. 21 and 23 into Eqn. 6. Here, the form of  $F_T$  is given by Eqn. 19.

Is it necessary to carry the thermodynamic potential factor  $F_T$  when predicting the rate of methanogenesis in the hydrothermal system? We can answer this question by comparing the rate predicted by the new rate law (Eqn. 24) with that suggested by the Monod equation

$$r = k[\text{X}] \frac{[\text{H}_2]}{[\text{H}_2] + K'_D} \quad (25)$$

which has been applied widely to describe rates of methanogenesis in both pure culture and natural sediments (Kristjansson et al., 1982; Lovley et al., 1982; Robinson and Tiedje, 1984; J. Oude Elferink et al., 1984). In this equation,  $K'_D$  is the half-saturation constant.

To focus on the effect of  $F_T$ , we take the representation of  $F_A$  in Eqn. 24 to be one, and carry the term  $K_D[\text{H}^+]$  as the half-saturation constant  $K'_D$ . In this way, the new rate law simplifies to

$$r = k[\text{X}] \frac{[\text{H}_2]}{[\text{H}_2] + K'_D} F_T \quad (26)$$

which is the product of the Monod equation and thermodynamic potential factor  $F_T$ . In reality, of course, the neglected concentrations may play important roles in controlling the respiration rate.

The product  $k[\text{X}]$ , which appears in both the Monod equation

and new rate law (Eqns. 25 and 26), represents the maximum rate of methanogenesis. This is the rate under optimum conditions, where the energy available is abundant relative to that conserved and substrate concentrations are large enough that both  $F_D$  and  $F_A$  approach unity. To assess the difference between predictions of the two rate laws, we therefore compute respiration rates relative to the maximum rate, as  $r(k[X])^{-1}$ . In evaluating Eqns. 25 and 26, we take the value of  $K'_D$  to be 2  $\mu\text{M}$ , within the range of  $K'_D$  reported for various methanogens and for methanogenesis in natural sediments (Widdel, 1988).

As shown in Figure 6, rates of methanogenesis predicted by Eqn. 26 and by the Monod equation show broadly different patterns. According to the Monod equation, the rate decreases slightly during mixing, but remains close to the maximum. The rate predicted by the new rate law, however, increases from zero in the unmixed hydrothermal fluids, approaching maximum rate at a mass ratio of about two parts seawater to one part hydrothermal fluid.

The differences between the rates predicted arise from the effect of the thermodynamic potential factor, which is absent in the Monod equation (Eqn. 25). The Monod rate is greatest in the unmixed hydrothermal fluid, in which the dihydrogen concentration is highest, and decreases slightly as the addition of seawater dilutes the dihydrogen. Over the mixing range considered, the dihydrogen concentration remains large relative to the value assumed for  $K'_D$ , so the rate predicted by the Monod equation varies little.

The new rate law (Eqns. 19 and 26) accounts for the effects of both dihydrogen concentration and the energy available. As discussed previously, the thermodynamic control on microbial respiration requires that for methanogenesis to proceed, the energy available in the environment must be greater than that needed to synthesize ATP, in which case  $-\Delta G_{\text{redox}} > 11 \text{ kJ}(\text{mol H}_2)^{-1}$ . In the unmixed hydrothermal fluid, little energy is available because  $-\Delta G_{\text{redox}}^\circ$  is small; the energy available amounts to little more than  $10 \text{ kJ}(\text{mol H}_2)^{-1}$ . As a result, the thermodynamic driving force and predicted respiration rate are close to zero, even though the dihydrogen concentration is high.

As seawater begins to mix into the hydrothermal fluid, the drop in temperature increases the available energy. Values of  $F_T$  and the predicted rate increase, even though the dihydrogen concentration is decreasing. After the mass ratio of seawater to fluids increases to  $\sim 2$ , the energy available increases above  $26 \text{ kJ}(\text{mol H}_2)^{-1}$ , leading to a value of  $F_T$  close to one. Now the rates predicted by the new rate law approach those predicted by the Monod equation. This example illustrates an important point. The Monod equation may work well where energy available ( $-\Delta G_{\text{redox}}$ ) is abundant relative to the amount conserved ( $m \Delta G_p$ ), but can give broadly erroneous results where the energy available is limited, as is the case in many geochemical environments.

### 5.3. Sulfate Reduction

In a mixture of seawater and seafloor hydrothermal fluid, sulfate reducing bacteria can reduce sulfate from seawater to sulfide by oxidizing acetate ( $\text{CH}_3\text{COO}^-$ ,  $\text{Ac}^-$ ) from the hydrothermal fluid. The redox reaction in this case is

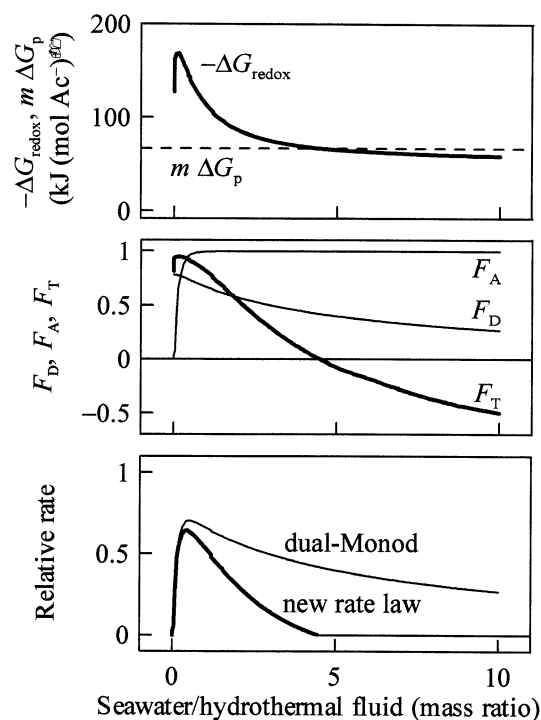


Fig. 7. Variation in the energy available  $-\Delta G_{\text{redox}}$ , thermodynamic potential factor  $F_T$ , kinetic factors  $F_D$  and  $F_A$ , and relative respiration rate for acetotrophic sulfate reduction during mixing of seawater with a seafloor hydrothermal fluid. The dashed line indicates the energy conserved ( $m \Delta G_p$ ). The value of  $F_T$  is evaluated using Eqn. 15;  $F_D$  and  $F_A$  are evaluated by Eqns. 25 and 32, respectively, and respiration rates are predicted using dual-Monod equation (Eqn. 34) and the new rate law (Eqn. 35). In evaluating Eqns. 34 and 35, we neglect the effect of  $[\text{H}^+]$ ,  $[\text{CO}_2]$ , and  $[\text{H}_2\text{S}]$  on respiration rate and take the value of  $K'_D$  and  $K'_A$  to be  $5 \times 10^{-3} \text{ mM}$  and  $5 \times 10^{-2} \text{ mM}$ , respectively. The predicted rates are expressed as a ratio, relative to  $k[X]$ .



since most sulfide and carbonate in the acidic hydrothermal fluid are present as  $\text{H}_2\text{S}$  and  $\text{CO}_2$ , respectively. The energy available ( $-\Delta G_{\text{redox}}$ ) to drive sulfate reduction depends on the standard Gibbs free energy change  $\Delta G_{\text{redox}}^\circ$ , temperature, pH, and the concentrations of  $\text{Ac}^-$ ,  $\text{CO}_2$ , sulfate and sulfide (Eqn. 14).

As seawater mixes into the hydrothermal fluid, the decrease in temperature causes the standard Gibbs free energy change to increase (i.e.,  $\Delta G_{\text{redox}}^\circ$  becomes less negative), as shown in Figure 5. At the same time, pH rises and  $\text{Ac}^-$  concentration falls during mixing (Fig. 5), serving to decrease the energy available to drive sulfate reduction. The decrease in sulfide and increase in sulfate concentration, conversely, works to increase the energy available. As shown in Figure 7, the energy available to drive sulfate reduction first increases during mixing, due to the effect of increasing sulfate concentration and decreasing sulfide concentration. After reaching a maximum at a seawater to hydrothermal fluid ratio of less than 0.1, the energy available begins to decrease sharply, as the effect of decreasing temperature becomes dominant.

Assuming that sulfate reducing bacteria conserve 4/3 ATP per turnover of reaction 27 (i.e.,  $m = 4/3$ ), and taking the value



of  $\chi$  as 1 per electron transferred or 8 per acetate oxidized, the thermodynamic potential factor takes the form

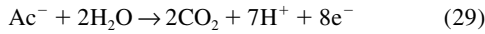
$$F_T = 1 - \exp\left(\frac{\Delta G_{\text{redox}} + \frac{4}{3}\Delta G_p}{8RT}\right) \quad (28)$$

Taking the phosphorylation potential  $\Delta G_p$  as  $50 \text{ kJ mol}^{-1}$ , the amount of energy conserved,  $m\Delta G_p$ , is  $\sim 66.7 \text{ kJ (mol Ac}^{-})^{-1}$ . From Eqn. 28, for  $F_T$  to approach unity, the thermodynamic driving force must be larger than  $150 \text{ kJ mol}^{-1}$ , or the energy available ( $-\Delta G_{\text{redox}}$ ) must be at least  $217 \text{ kJ mol}^{-1}$ .

The calculation results (Fig. 7), however, suggest that during mixing the driving force never exceeds  $200 \text{ kJ (mol Ac}^{-})^{-1}$ , so the thermodynamic potential factor  $F_T$  is invariably less than one. The value of  $F_T$  first increases during mixing and then decreases, reflecting variation in the energy available ( $-\Delta G_{\text{redox}}$ ) to drive sulfate reduction. When the energy available no longer exceeds that needed to synthesize ATP, the thermodynamic drive and hence  $F_T$  turn negative. A negative thermodynamic drive would hydrolyze ATP to ADP and  $P_i$  and drive electrons backward through the respiratory chain, in this case causing sulfide oxidation. To avoid dissipation of ATP store, microorganisms would regulate the redox enzymes to interrupt its respiratory chain. In other words, the rate can reasonably be taken as zero where the energy available is insufficient to support ATP synthesis.

#### 5.4. Rate of Sulfate Reduction

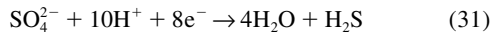
To evaluate the rate of sulfate reduction, we write the general rate expression as we did for methanogenesis. From the electron donating half-reaction



and Eqn. 4,  $F_D$  can be written as

$$F_D = \frac{[\text{Ac}^{-}]}{[\text{Ac}^{-}] + K_D[\text{H}^{+}][\text{CO}_2]} \quad (30)$$

From the electron accepting half-reaction



and Eqn. 8,  $F_A$  is

$$F_A = \frac{[\text{SO}_4^{2-}][\text{H}^{+}]}{[\text{SO}_4^{2-}][\text{H}^{+}] + K_A[\text{H}_2\text{S}]} \quad (32)$$

Combining Eqns. 28, 30, and 32 leads to

$$r = k[\text{X}] \frac{[\text{Ac}^{-}]}{[\text{Ac}^{-}] + K_D[\text{H}^{+}][\text{CO}_2]} \times \frac{[\text{SO}_4^{2-}][\text{H}^{+}]}{[\text{SO}_4^{2-}][\text{H}^{+}] + K_A[\text{H}_2\text{S}]} F_T \quad (33)$$

This is the general rate expression for microbial sulfate reduction using dihydrogen as electron donor. In practice, the dual-Monod equation (Widdel, 1988)

$$r = k[\text{X}] \frac{[\text{Ac}^{-}]}{[\text{Ac}^{-}] + K'_D} \frac{[\text{SO}_4^{2-}]}{[\text{SO}_4^{2-}] + K'_A} \quad (34)$$

is commonly used to describe the rate of microbial sulfate reduction (e.g., Nedwell, 1982; Ramm and Bella, 1974). Here,  $K'_D$  and  $K'_A$  are half-saturation constants. To compare the predictions of the two rate expressions, we neglect the effects of  $[\text{H}^{+}]$ ,  $[\text{CO}_2]$  and  $[\text{H}_2\text{S}]$  in the new rate law, giving

$$r = k[\text{X}] \frac{[\text{Ac}^{-}]}{[\text{Ac}^{-}] + K'_D} \frac{[\text{SO}_4^{2-}]}{[\text{SO}_4^{2-}] + K'_A} F_T \quad (35)$$

We employ a form of the new rate law, therefore, that is the product of the dual-Monod equation and thermodynamic potential factor  $F_T$ . Here,  $K'_D$  and  $K'_A$  are products of  $K_D[\text{H}^{+}][\text{CO}_2]$  and  $K_A[\text{H}_2\text{S}][\text{H}^{+}]^{-1}$ , respectively. In evaluating Eqns. 34 and 35, we take values of  $5 \mu\text{M}$  and  $50 \mu\text{M}$ , respectively, for  $K'_D$  and  $K'_A$ . These values are within the ranges reported for sulfate reducing bacteria and sulfate reduction in natural sediments (Widdel, 1988).

The rate of sulfate reduction predicted by the new rate law differs from that resulting from the dual-Monod equation, as shown in Figure 7. Initially, the rate predicted by either rate law is near zero because there is little sulfate in the hydrothermal fluid. As the fluid mixes with seawater, the sulfate added serves to increase the value of  $F_A$ , whereas the decrease in acetate concentration decreases the value of  $F_D$ . During the initial mixing, for seawater to hydrothermal fluid ratios less than  $\sim 0.2$ , the effect of increasing sulfate concentration dominates and the rate increases. Once the sulfate concentration exceeds the value of  $K'_A$  ( $50 \mu\text{M}$ , in this example),  $F_A$  approaches unity and the effect of increasing sulfate concentration becomes minimal. At this point, the rate starts to decrease due to the decline in acetate concentration.

The rate predicted by the new rate law decreases much more sharply with mixing than that given by the dual-Monod equation, due to the effect of the thermodynamic potential factor. At mass ratios less than about one, the energy available ( $-\Delta G_{\text{redox}}$ ) remains relatively high and the value of  $F_T$  is near one. The thermodynamic control under these conditions is not significant and the rates predicted by the two rate laws are similar. At mass ratios exceeding about two, the energy available decreases quickly, as does the value of  $F_T$ . The rate predicted by the new rate law falls sharply to zero. At a mass ratio of  $\sim 4.5$ , the energy available drops below the amount of energy needed to synthesize ATP. At this point, the value of  $F_T$  decreases to zero and respiration cannot proceed. The dual-Monod equation, in contrast, predicts that respiration will continue during mixing, even though the energy available is no longer sufficient to support the metabolism.

## 6. DISCUSSION

We propose in this paper to use a rate law of general form to develop rate expressions for microbial respiration in geochemical environments. The new rate law (Eqns. 6, 7, 8, and 9) differs from laws in common use today (Table 3) in that it accounts for the effects of energy availability and for all of the chemical species in the redox reaction. The new rate law is derived on the basis of the mechanism of microbial respiration

Table 3. Rate equations in common use and conditions under which they represent simplifications of the rate law presented.

Rate equation <sup>a</sup>	[X]	$F_D$	$F_A$	$F_T$
Dual Monod equation $r = k[X] \frac{[D]}{[D] + K'_D} \frac{[A]}{[A] + K'_A}$				1
Monod equation $r = k[X] \frac{[D]}{[D] + K'_D}$			Constant	1
Michaelis-Menten equation $r = k' \frac{[D]}{[D] + K'_D}$	Constant		Constant	1
Logistic equation $r = k[D](C - [D])^b$		$[D] \ll K'_D$	Constant	1
First order equation $r = k[D]$	Constant	$[D] \ll K'_D$	Constant	1
Logarithmic equation $r = k(C - [D])^b$		$[D] \gg K'_D$	Constant	1
Zero order equation $r = k'$	Constant	$[D] \gg K'_D$	Constant	1

<sup>a</sup> In each case, no more than one chemical species in the electron donating reaction and one in the accepting reaction can vary in concentration.

<sup>b</sup>  $C = \nu_D [X]_0 / Y + [D]_0$ . Here  $[X]_0$  and  $[D]_0$  are initial concentrations of biomass and electron donor.

(Jin and Bethke, 2002), i.e., how electrons are transferred through the respiratory chain and how the energy is conserved by synthesizing ATP. Factors such as the need of the microorganism to derive and conserve energy and the concentrations of electron donor, acceptor, and reaction product species are incorporated in the new law, in the expression of thermodynamic potential factor  $F_T$  and kinetic factors  $F_D$  and  $F_A$ .

The thermodynamic potential factor  $F_T$  is a nonlinear function of the thermodynamic driving force, the difference between the energy available and the energy conserved to synthesize ATP. Where the energy available is much larger than that conserved, the value of  $F_T$  approaches unity. Under such circumstances, the thermodynamic control can be neglected in calculating microbial respiration rates. This is the case, as we have shown, for aerobic respiration and denitrification using dihydrogen as electron donor. Where the energy available is of similar magnitude to that conserved, as in the case of sulfate reduction and methanogenesis, the thermodynamic driving force is small and the value of  $F_T$  is commonly less than unity. In other words, the energy available limits the rate of respiration and  $F_T$  has to be considered to predict correctly the rate of respiration. Where the energy available balances the amount conserved, the driving force decreases to zero and microbial respiration reaches the state of thermodynamic equilibrium. The value of  $F_T$  at this point becomes zero, as does the rate of respiration. Where the energy available falls below the amount needed to synthesize ATP, the driving force and thermodynamic potential factor turn negative. Under such conditions, the new law would predict a negative rate; i.e., respiration would proceed backwards. To prevent reverse electron transfer through the respiratory chain and the loss of its ATP stores, a microorganism can regulate the activities of redox enzymes to interrupt its respiration.

Rate laws in common use today to describe microbial respiration are chosen and parameterized by fitting the rate expression to a given experimental data set. The standard for justifying the use of a particular rate expression is solely empiric; i.e., how closely the rate expression can fit experimental observations. As a result, more than one rate law has been used to describe the respiration of an individual strain, as in the case of aerobic benzoate degradation (Simkins and Alexander, 1984). From the perspective of chemical kinetics, however, the form of the rate law should depend only on the reaction mechanism of the respiration process.

The new rate law is a generalization of the various empiric rate equations in common use, and hence honors this perspective. It can be applied in the general case, or simplified to the forms of the other laws under specific sets of conditions. In other words, each of the commonly used rate laws is a specific simplification of the new law we developed. These simplifications are summarized in Table 3. Taking microbial sulfate reduction as an example, we have seen that once the electron donating and accepting half-reactions are specified, the new rate law assumes a manageable form (Eqn. 33). Where the energy available ( $-\Delta G_{\text{redox}}$ ) for sulfate reduction is much larger than the energy saved ( $m \times \Delta G_p$ ), the driving force is large and the value of  $F_T$  approaches unity. Under such conditions, the rate expression (Eqn. 33) reduces to

$$r = k[X] \frac{[\text{Ac}^-]}{[\text{Ac}^-] + K_D[\text{H}^+][\text{CO}_2]} \frac{[\text{SO}_4^{2-}][\text{H}^+]}{[\text{SO}_4^{2-}][\text{H}^+] + K_A[\text{H}_2\text{S}]} \quad (36)$$

Assuming  $[\text{H}^+]$ ,  $[\text{CO}_2]$ , and  $[\text{H}_2\text{S}]$  remain constant, as in the case where pH is buffered, dissolved carbon dioxide is in balance with atmospheric  $\text{CO}_2$ , and  $[\text{H}_2\text{S}]$  is limited by metal

concentrations in the environment, the rate expression simplifies to the dual-Monod equation (Eqn. 34). Where  $[\text{SO}_4^{2-}]$  is much larger than  $K'_A$ , as would be the case where  $[\text{HS}^-]$  is small, the value of  $F_A$  approaches unity. The sulfate concentration in seawater,  $\sim 28$  mM (Drever, 1988), is considerably larger than  $K'_A$  values determined in experimental studies (Smith and Klug, 1981; Ingvorsen and Jorgensen, 1984; Ingvorsen et al., 1984) for sulfate reducers; these values vary from 5 to 220  $\mu\text{M}$ . In this case, the rate expression (Eqn. 36) takes the form of the Monod equation.

The rate laws in common use may be expected to work well for describing laboratory experiments, where only one or two factors may be allowed to vary, and where a large thermodynamic driving force is likely maintained. The extrapolation of experimental studies as models of actual geochemical environments, however, presents a special challenge, because many factors control respiration in the field. Predicting the rate of microbial respiration in the field can be expected to require a rate expression of general form that accounts for a variety of controlling factors, including energy availability and concentrations of substrates and metabolic products.

*Acknowledgments*—We thank James Imlay, Matthew Kirk, and Robert Sanford for their interest and generous advice. This work was supported by Department of Energy Grant DE-FG02-02ER15317 and the generosity of Chevron, ConocoPhillips, ExxonMobil Upstream Research, Idaho National Engineering and Environmental Laboratory, Lawrence Livermore, Sandia, SCK-CEN, Texaco, and the U.S. Geological Survey.

*Associate editor:* K. L. Nagy

## REFERENCES

- Bethke C. M. (1996) *Geochemical Reaction Modeling*. Oxford University Press.
- Bethke C. M. (2002) *The Geochemist's Workbench, Release 4.0*. University of Illinois.
- Deppenmeier U., Muller V., and Gottschalk G. (1996) Pathways of energy conservation in methanogenic archaea. *Arch. Microbiol.* **165**, 149–163.
- Drever J. I. (1988) *The Geochemistry of Natural Waters*. Prentice-Hall.
- Erecinska M. and Wilson D. F. (1982) Regulation of cellular energy metabolism. *J. Membrane Biol.* **70**, 1–14.
- Huber C. and Wächtershäuser G. (1997) Activated acetic acid by carbon fixation on (Fe,Ni)S under primordial conditions. *Science* **276**, 245–247.
- Ingvorsen K. and Jorgensen B. B. (1984) Kinetics of sulfate uptake by freshwater and marine species of *Desulfovibrio*. *Arch. Microbiol.* **139**, 61–66.
- Ingvorsen K., Zehnder A. J. B., and Jorgensen B. B. (1984) Kinetics of sulfate and acetate uptake by *Desulfobacter postgatei*. *Appl. Environ. Microbiol.* **47**, 403–408.
- Jannasch H. W. and Mottl M. J. (1985) Geomicrobiology of deep-sea hydrothermal vents. *Science* **229**, 717–725.
- Jin Q. and Bethke C. M. (2002) Kinetics of electron transfer through the respiratory chain. *Biophysical Journal* **83**, 1797–1808.
- Jin Q. and Bethke C. M. (2003) A new rate law describing microbial respiration. *Appl. Environ. Microbiol.* **69**, 2340–2348.
- Jones W. J., Leigh J. A., Mayer F., Woese C. R., and Wolfe R. S. (1983) *Methanococcus jannaschii* sp. nov., an extremely thermophilic methanogen from a submarine hydrothermal vent. *Arch. Microbiol.* **136**, 254–261.
- Kashefi K., Holmes D. E., Baross J. A., and Lovley D. R. (2003) Thermophilily in the Geobacteraceae: *Geothermobacter ehrlichii* gen. nov., sp. nov., a novel thermophilic member of the Geobacter-

- aceae from the “Bag City” hydrothermal vent. *Appl. Environ. Microbiol.* **69**, 2985–2993.
- Kristjansson J. K., Schonheit P., and Thauer R. K. (1982) Different  $K_s$  values for hydrogen of methanogenic bacteria and sulfate reducing bacteria: An explanation for the apparent inhibition. *Arch. Microbiol.* **131**, 278–282.
- Lovley D. R., Dwyer D. F., and Klug M. J. (1982) Kinetic analysis of competition between sulfate reducers and methanogen for hydrogen in sediment. *Appl. Environ. Microbiol.* **43**, 1373–1379.
- Lovley D. R. and Goodwin S. (1988) Hydrogen concentrations as an indicator of the predominant terminal electron-accepting reactions in aquatic sediments. *Geochim. Cosmochim. Acta* **52**, 2993–3003.
- Masel R. I. (2001) *Chemical Kinetics and Catalysis*. Wiley-Interscience.
- McCollom T. M. and Shock E. L. (1997) Geochemical constraints on chemolithoautotrophic metabolism by microorganisms in seafloor hydrothermal systems. *Geochim. Cosmochim. Acta* **61**, 4375–4391.
- McKay A., Quilter J., and Jones C. W. (1982) Energy conservation in the extreme thermophile *Thermus thermophilus* HB8. *Arch. Microbiol.* **131**, 43–50.
- Mitchell P. (1961) Coupling of phosphorylation to electron and hydrogen transfer by a chemi-osmotic type of mechanism. *Nature* **191**, 144–148.
- Nedwell D. B. (1982) The cycling of sulphur in marine and freshwater sediments. In *Sediment Microbiology* (eds. D. B. Nedwell and C. M. Brown), pp. 73–106. Academic Press.
- Nethe-Jaenchen R. and Thauer R. K. (1984) Growth yields and saturation constants of *Desulfovibrio vulgaris* in chemostat culture. *Arch. Microbiol.* **137**, 236–240.
- Oude Elferink S.J.W.H., Visser A., Hulshoff Pol L. W., and Stams A. J. M. (1994) Sulfate reduction in methanogenic bioreactors. *FEMS Microbiol. Rev.* **15**, 119–136.
- Ramm A. E. and Bella D. A. (1974) Sulfide production in anaerobic microcosms. *Limnol. Oceanogr.* **19**, 110–118.
- Reysenbach A.-L., Longnecker K., and Kirshtein J. (2000) Novel bacterial and archaeal lineages from an in situ growth chamber deployed at a mid-Atlantic Ridge hydrothermal vent. *Appl. Environ. Microbiol.* **66**, 3798–3806.
- Robinson J. A. and Tiedje J. M. (1984) Competition between sulfate-reducing and methanogenic bacteria for H<sub>2</sub> under resting and growing conditions. *Arch. Microbiol.* **137**, 26–32.
- Simkins S. and Alexander M. (1984) Models for mineralization kinetics with the variables of substrate concentration and population density. *Appl. Environ. Microbiol.* **47**, 1299–1306.
- Smith R. L. and Klug M. J. (1981) Reduction of sulfur compounds in the sediments of a eutrophic lake basin. *Appl. Environ. Microbiol.* **41**, 1230–1237.
- Stevens T. O. and Mckinley J. P. (1995) Lithoautotrophic microbial ecosystems in deep basalt aquifers. *Science* **270**, 450–454.
- Stouthamer A. H. (1991) Metabolic regulation including anaerobic metabolism in *Paracoccus denitrificans*. *J. Bioenergetics Biomembranes* **23**, 163–185.
- Thauer R. K., Jungermann K., and Decker K. (1977) Energy conservation in chemotrophic anaerobic bacteria. *Bacteriol. Rev.* **41**, 100–180.
- Trumpower B. L. (1990) The protonmotive Q cycle: Energy transduction by coupling of proton translocation to electron transfer by the cytochrome bc<sub>1</sub> complex. *J. Biol. Chem.* **265**, 11409–11412.
- van Verseveld H. W. and Bosma G. (1987) The respiratory chain and energy conservation in mitochondrion-like bacterium *Paracoccus denitrificans*. *Microbiol. Sci.* **4**, 329–333.
- White D. (1995) *The Physiology and Biochemistry of Prokaryotes*. Oxford University Press.
- Widdel F. (1988) Microbiology and ecology of sulfate- and sulfur-reducing bacteria. In *Biology of Anaerobic Microorganisms* (ed. A. J. B. Zehnder), pp. 469–585. Wiley.

## APPENDIX

### SUPPLEMENTARY DATA

Supplementary data associated with this article can be found, in the online version, at doi:10.1016/j.gca.2004.08.010.